

Cite this: DOI: 00.0000/xxxxxxxxxx

Torque about electrostatically charged spheres makes them more attractive

Michael R. Swift,^a Mike I. Smith^{*a}

Received Date

Accepted Date

DOI: 00.0000/xxxxxxxxxx

The strength of interparticle interactions in a granular system controls how a collection of insulating particles flow, cohere and fragment. Forces due to electrostatic charging, particularly in free-fall or low gravity environments, can dominate the static and dynamic interactions with important implications for understanding natural and industrial processes. Here we show that shaking of homogeneous, spherical particles can result in a non-uniform surface charge distribution. The measured dipole moment and torque for each particle are found to be strongly correlated. However, our model shows that to predict the torque and force requires one to consider the full surface charge distribution. This overlooked torque is not only significant, but would amplify attractive interactions through particle reorientation.

1 Introduction

Electrostatic charging underlies many natural phenomena such as the coalescence of ice particles in thunder clouds¹, agglomeration of volcanic ash², and reshaping of sand dunes by the wind³. In industry charge is harnessed to separate materials^{4–6} but also causes significant challenges in fluidized bed reactors⁷ and in ensuring homogeneously distributed ingredients in pharmaceutical tablets⁸. In all cases, the strength of electrostatic interparticle interactions affects the response to applied stress - flow, cohesion or fragmentation - making it a vital input to a full understanding of such processes.

These forces are also particularly pronounced in space: the thin atmosphere or vacuum inhibits charge dissipation^{9,10}; competing gravitational forces are weaker^{10,11}, and additional charging mechanisms exist due to solar winds^{12,13}. As a result charged space dust, encountered during the Apollo missions, is still a serious concern for maintaining technology in space and safeguarding astronauts' health^{12,14–16}. Furthermore, free-fall experiments on Earth have highlighted the potential importance of additional forces involved in the early stages of planet formation: charged particles can induce a dipole in one another, enabling like-charged particles to stick together^{17,18}.

In a demonstration that can be done at home, when two different materials are rubbed together, they charge. The expected polarity of each material is denoted by its relative position in the triboelectric series¹⁹. Yet current research exposes this as a drastic oversimplification. Firstly, the task of taking reproducible

measurements is fraught with difficulty¹⁹. Secondly, the literature is full of surprises: the polarity of materials can depend on the applied strain²⁰ or the ambient humidity²¹; materials that initially charge negatively, may subsequently charge positively²²; even charge conservation may apparently be broken, with both materials charging positively²³.

In an experiment of a specific particle bouncing on a planar surface, made from the same high purity SiO₂, each consistently charged in opposite directions²⁴. In repeat experiments, the polarity of each surface appeared to vary randomly, implying that the charge density does not average out over macroscopic length scales. Following a single bounce of an initially neutral ball, it is self-evident that the macroscopic surface charge distribution will be inhomogeneous. However, simulations assuming many random collisions showed that the large scale surface charge density quickly becomes quasi-uniform^{25,26}. Under this assumption, interactions due to the charge distribution can be adequately approximated by an equivalent central charge^{5,17,18,25–27}.

However, if a macroscopic, *non-uniform* charge distribution can exist on the surface of a bouncing sphere, it could modify forces and generate torques. In this article we address the following questions: can such a charge distribution be easily generated, and if so, are the interparticle forces and torques strong enough to matter?

2 Results and Discussion

2.1 Inhomogeneous surface charge

In our initial experiments we demonstrate that simple shaking of spherical particles produces a permanent non-uniform distribution of charge over the particle surface. Ten clean beads (see supplementary information), polypropylene (PP) or PTFE (diam-

^aSchool of Physics and Astronomy, University of Nottingham, Nottingham NG7 2RD, UK E-mail: mike.i.smith@nottingham.ac.uk

† Electronic Supplementary Information (ESI) available: [details of any supplementary information available should be included here]. See DOI: 00.0000/00000000.

eters 4 and 3 mm respectively), are shaken vertically (freq=40Hz, acc=3.75g) in a clean glass container using an electromagnetic shaker. Initially, the particles bounce violently but as the particles charge their mean height gradually reduces until they eventually stick to the container. An aluminium block, covered with a thin glass coverslip ($50 \times 24\text{mm}^2$) is placed in a holder mounted on a DC motor enabling the angle ϕ to be slowly altered (figure 1a). With $\phi \sim 0^\circ$ we gently tip a bead from the container onto the coverslip. Whilst some beads roll off the uncharged surface ($\sim 50\%$), many surprisingly stick. We then slowly tilt the surface. The beads often roll a fraction of a bead diameter before eventually rolling off the surface at an angle ϕ_{\max} (supplementary video 1). ϕ_{\max} varies between beads but is always a substantial angle (figure 1b).

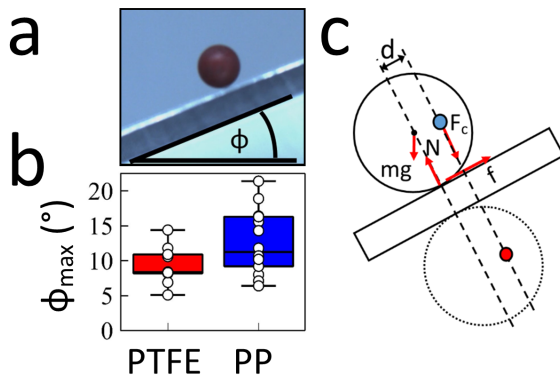


Fig. 1 a) A charged particle on a glass coverslip above an aluminium block. b) ϕ_{\max} for PTFE and PP particles. The whiskers represent the full data range, the boxes represent the lower and upper quartile of the data. Individual results are marked with points. c) Schematic of the charged particle interacting with its image charge.

With $\phi \sim 0^\circ$ we performed two control experiments. Firstly, using uncharged beads we confirmed that the interaction is solely due to charge. Secondly, removing the aluminium block, we tipped charged beads onto the coverslip, confirming the dominant interaction is with the metal and not the glass. In both cases all the beads immediately rolled off. Using insulated tweezers to manually place beads on the glass produced the same result.

For an *uncharged* bead not to roll, the torque due to friction must be balanced by the moment of the normal force about the centre of mass. This moment is due to the slight deformation at the point of contact (rolling friction). The bead therefore rolls at a very small angle²⁸. While a charged particle may cling to a charged surface, in these experiments only the bead is charged. However, due to the aluminium block the bead has additional interactions with its own image charge (figure 1c). For a uniformly charged spherical bead there would be no additional torque since the net Coulomb force, and any induced polarization force, act along the line joining the centres of the bead and its image. Therefore, as for the uncharged bead it would roll easily. Figure 1c depicts an inhomogeneous charge distribution shown schematically by a single non-central charge. This charge produces a torque balancing the couple caused by friction and significantly increases the angle ϕ_{\max} at which the bead rolls. This simple

observation indicates: 1) simply shaking spheres can counter-intuitively result in a non-uniform surface charge distribution 2) the generated torques do matter.

2.2 Quantifying the dipole on electrostatically charged spheres

Using an alternative approach, we now quantify how the distribution of charge can be related to the strength of particle interactions; measuring how the charge and dipole moment relate to the torque. We use 10mm diameter spheres of PTFE and PP with a 1.5mm diameter hole. Three beads were cleaned (see supplementary information), picked up on the ends of insulated tweezers, dried with N₂ and then placed into a sealed glass container. This was then shaken for 5 minutes at 3.75g. A few beads were shaken longer (30 mins) and harder ($\sim 5.25\text{g}$), but no differences were observed. During shaking, the beads charge rapidly as they collide predominantly with the walls of the container without sticking.

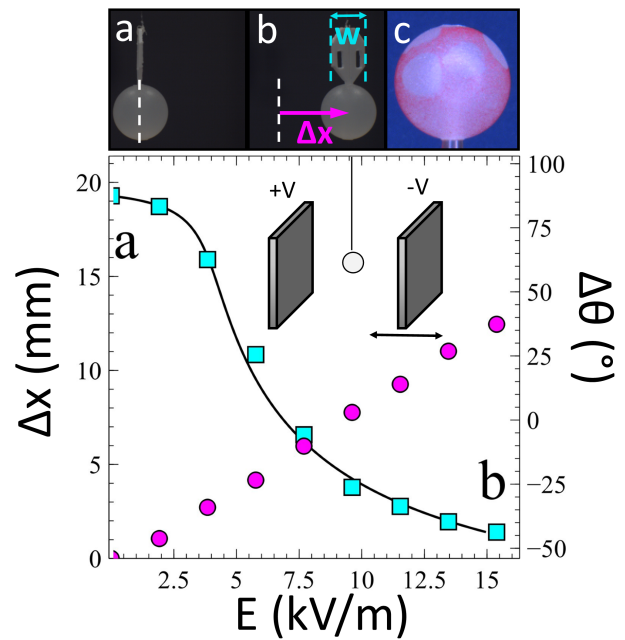


Fig. 2 A charged particle is suspended in a uniform electric field. As the field is increased the particle is displaced by $\Delta x(\circ)$ which is used to measure the particle's total charge. Due to the non-uniform charge distribution, it experiences a torque, resulting in rotation shown in the top panel (a,b). The change in orientation $\Delta\theta(\square)$ can be calculated from the projected width W . The black line (main panel) is a fit to equation 1. c) The non-uniform surface charge distribution can be observed qualitatively using charged toner.

After charging, beads are retrieved from the container by inserting the ends of discharged tweezers into the hole. Allowing the tips of the tweezers to spring open, the bead can be lifted without applying downwards pressure. A tag (figure 2a,b), fixed to a fibre of length L , is inserted into the other end. The fibre, attached to a puck, is used to suspend the bead between two large aluminium capacitor plates separated by a distance d in a perspex

cabinet purged with dry air ($\text{RH} \sim 25\%$). We emphasise that no contact is made at any stage with the outer surface of the bead.

To measure the charge, Q , on a bead of mass m (figure 2), the voltage, V , across the capacitor plates is incrementally increased, and the displacement $\Delta x(\square)$ measured from corresponding images. The charge $Q \approx mgd\Delta x/LV$ can vary between ~ 1 and 10nC . The PTFE beads charge negatively, whilst the PP beads charge positively.

As the electric field strength is increased the bead also rotates, indicating an uneven charge distribution across its surface. It has been proposed that charge could migrate across surfaces in nanolayer water films under an electric field²⁹. However, in our experiments, the orientation of the bead remains constant at a fixed voltage, indicating the surface charges are immobile.

The dipole moment of the charge distribution is a vector at some angle to the vertical with a projection (P) onto the horizontal plane. In the presence of a horizontal electric field (E) this results in a torque (τ) about the vertical axis. This is counteracted by the torsional stiffness (K) in the fibre yielding the torque balance equation:

$$E = \frac{K\Delta\theta}{P\sin(\theta_0 + \Delta\theta)}, \quad (1)$$

where θ_0 is the angle of the projected dipole moment at $E=0$, and $\Delta\theta$ is the rotation of the bead. The measured angle of the bead θ , can be extracted from the apparent width, $W = |l\cos(\theta)| + |t\sin(\theta)|$, of the tag in the acquired images (figure 2b), where l is the actual width and t the thickness of the tag. Figure 2 shows how the change in angle of the bead at different field strengths (\square) can be fit to equation 1 and used to extract the projected dipole moment.

Measurements of the dipole also show significant variation. That this is not an artefact of the measurement is clear, since beads that have not been shaken have charges too small to be measured ($< 1\text{pC}$), and a charged bead deposited in the glass container, then remeasured, results in the same value ($\pm 0.1\text{nC}$). This variation is also observed for multiple beads in the same experiment and a single bead measured in multiple experiments. This indicates that the final charge and dipole are not intrinsic properties of individual beads, arising from manufacturing differences or variations in material properties, but are altered by sample history²⁴.

After several measurements, we exposed beads to a cloud of photocopy toner. The toner was agitated in a sealed container, following which the bead was introduced on the tip of a pipette. Figure 2c shows the same bead whose data is plotted in the main panel. The bead exhibits several distinct regions that appear to have undergone minimal charging. Comparing the toner-covered areas they also appear to have different densities of toner particles. Beads measured with much smaller dipoles were found to result in much more uniform toner patterns. These qualitative observations indicate that the dipole measurement provides a quantitative measure of the charge distribution on the bead.

In addition to measurements on PTFE and PP beads we also used a few beads made from silicone, acrylic (painted and unpainted) and Delrin. When shaken and measured these beads

also exhibited strong dipoles. Even if our beads are not perfect, they illustrate the observational fact, that, under levels of scrutiny that far exceed those in industrial or natural processes, highly non-uniform charging often occurs.

Some recent studies have paid particular attention to the purity of samples and yet the charging of a surface in a particular experiment was still not predictable²⁴. Inhomogeneous surface charge density may also arise in other situations: liquid evaporation on a surface^{30,31}; fractoemission during grinding³²; charge transfer in electric fields^{33–36}. Laboratory experiments suggest that particles at the lunar surface may also be charged asymmetrically due to UV radiation or dusty plasmas¹³. More prosaically, distributions of surface charge would arise from such elementary considerations as inhomogeneously distributed impurities or aggregates composed of multiple charged species^{2,37}.

2.3 Measuring the torque of an inhomogeneously charged sphere

To understand the impact of non-uniform charging on the interaction of beads we directly measure the size of the resulting torques. After each charge and dipole measurement, we switch off the external field and allow the plates to discharge. One capacitor plate is covered with washed, discharged glass coverslips. The plate is mounted on a manual translation stage which allows it to be slowly moved towards the charged bead. When the bead is $\sim 3\text{cm}$ from the plate there is a noticeable attraction towards the metal. As the gap is decreased further, the force due to the image charge accelerates the bead towards the plate where it sticks (see figure 3a and supplementary video 2). The impact velocity depends upon charge, but we estimate it to be as high as 0.3ms^{-1} . The bead also rotates, demonstrating that the generated torque can influence the dynamical interactions between approaching particles.

Once the bead has come to rest, we move the plate until the fibre attached to the bead is vertical. We then rotate the puck, twisting the fibre in a clockwise direction (viewed from above). The torque applied to the bead is proportional to the angle rotated and the torsional spring constant of the fibre. Figure 3b shows that a charged bead makes some small movements in discrete steps but then at a critical torque $\sim 3.5\text{mNm}$ (15.5 revolutions of the puck) spins wildly off the glass (supplementary video 3). These measurements, therefore, demonstrate the same behaviour observed qualitatively in figure 1.

Each torque measurement is made immediately after the corresponding charge and dipole measurement. When the charge is plotted against the measured torque there is no apparent correlation (supplementary figure 2). However, there is a strong correlation between the measured dipole moment and torque. One might therefore ask whether a knowledge of a particle's charge and dipole moment, are sufficient to predict its interactions?

2.4 How spatial charge distributions affect particle interactions

Here we explore how an inhomogeneous surface charge distribution modifies the interactions between a spherical particle and

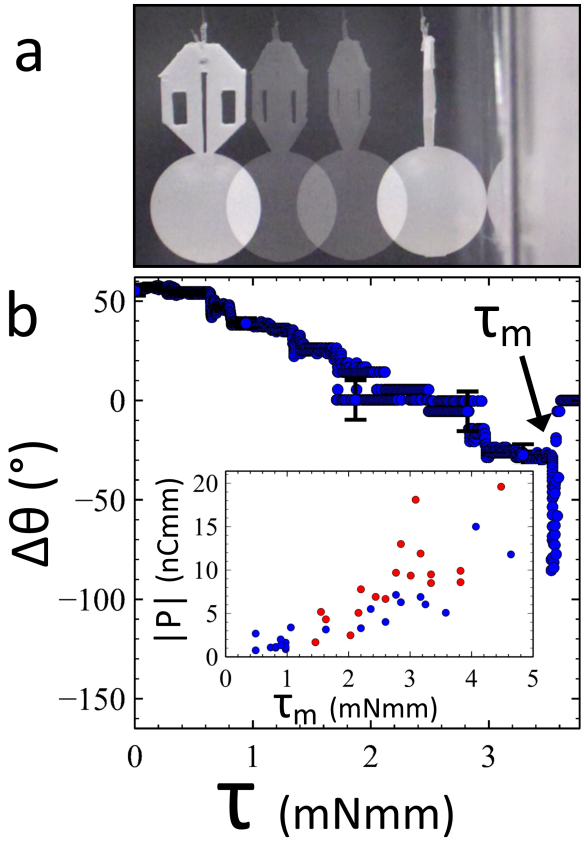


Fig. 3 Measuring the torque due to non-uniform charging. a) With the electric field switched off, the capacitor plate is moved towards the particle. At about 3cm separation, the particle experiences a strong attraction towards its own image charge and rotates.b) The change in angle $\Delta\theta$ as a torque τ is applied to the bead. The bead makes small discrete movements as the torque increases until it reaches a maximum (τ_m). Representative error bars are shown. Inset) Correlation between the measured dipole moment and torque of PTFE (red) and PP (blue) particles.

its own image. Using python we numerically evaluate a simple model to calculate the interparticle forces and torques at different orientations. We divide a typical total charge ($Q = 5\text{nC}$) equally between N point charges distributed at random over the surface of a 10mm diameter sphere. Increasing the number of points N provides a simple way to gradually make the charge distribution more uniform without changing the net charge. As per the experiment, the sphere interacts with its image, separated by a gap of 1mm (figure 4a and supplementary video 4). Rotating the sphere and its image, we calculate the varying normal force and torque about the vertical axis of the sphere. Each charge on the sphere experiences a Coulomb force with every image charge. The induced polarization is not considered¹⁷ as in our case the polarizability is small³⁸.

In the inset to Fig. 4, upper panel, as a function of orientation, we show the torque (red) for one distribution of $N = 20$ charges. We also plot the torque for the distribution's projected dipole moment, P (blue). The similarity between the blue and red curves

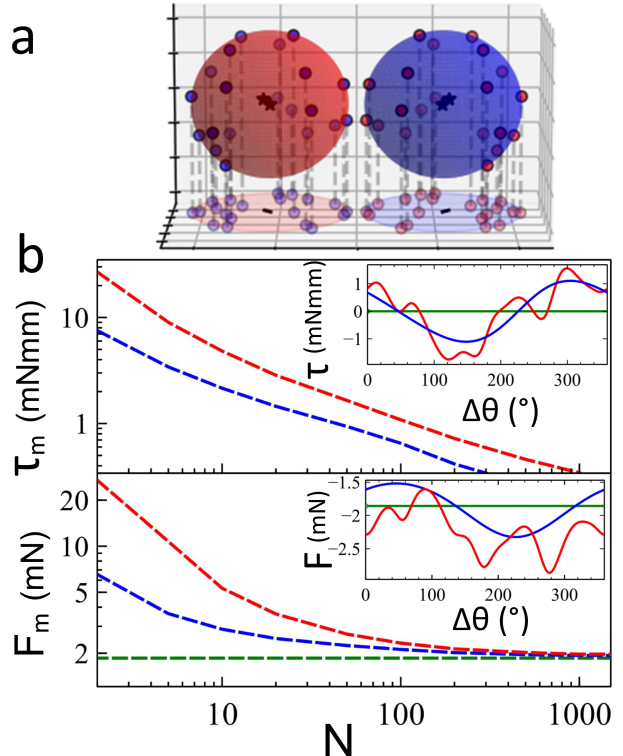


Fig. 4 a) An inhomogeneously charged sphere is modelled using N randomly positioned surface charges as described in the main text. b) The insets show the calculated torque and normal force of the sphere interacting with its image (red). We also calculate the interactions assuming all the charge is located centrally (green) and for the equivalent dipole moment (blue). The main panels show the median value of the absolute max torque (τ_m) and normal force (F_m).

gives cause for some optimism. However, supplementary figure 3 shows a different charge distribution for $N = 20$ in which the true torque is not well approximated, sometimes even predicting the wrong sign. Figure 4 upper main panel summarises the differences between the dipole approximation and the full charge distribution. The red line represents, for each value of N , the median of the max torque obtained in 500 independent charge distributions. The blue line represents the calculation for the equivalent dipole moment. Whilst the dipole moment is a significant improvement on the central charge ($\tau_m = 0$) approximation, it still underestimates the true torque by a considerable margin. We note that in the experiments a sphere with $Q = 5\text{nC}$ would be expected to have a dipole moment $\sim 5 - 15 \text{nCmm}$. Similar dipole moments in our model exist for $N \sim 10 - 50$. The model predicts $\tau_m \sim 1.5 - 7 \text{ mNm}$ which is comparable to the measured values.

One can also calculate the normal force between a particle and its image, Fig. 4, lower panel. The full charge distribution (red) predicts the attractive forces could be significantly more than expected due to either a uniform charge (green) or the dipole model (blue). If the particles are brought closer together, the deviation between the models would also increase. As our experiments show a significant torque tends to reorient particles resulting in larger than anticipated interparticle forces. One would therefore

expect that in clusters of oppositely charged particles inhomogeneous charging would strongly enhance the cohesive strength.

Recent research has demonstrated that the Coulombic interaction between particles can also result in induced dipoles¹⁷. Whilst not generating a torque between two particles, these forces can be large, enabling even like-charged particles to stick together. However, these forces are only relevant for materials with high polarizabilities / dielectric constants and / or large ratios between the particle charges³⁸. In contrast, permanent dipoles generate torques and would strongly modify inter-particle forces regardless of materials or charge ratio. Furthermore, a permanent non-uniform charge distribution would also modify the strength of any induced dipole.

3 Conclusions

Our results are important for both particle-surface and particle-particle interactions. Image charge effects at metal surfaces are known to be of importance in, for example, fluidised bed reactors⁷ and drum electrostatic separators⁵. Mixtures of oppositely charged particles occur not just in separating different materials^{5,6} but also in same-material charging^{17,33}. These additional torques would therefore be particularly relevant to phenomena such as aeolian transport and dune dynamics^{10,34}.

Our experiments show that the measured torques correspond to about 20% of the weight of a particle (on Earth) acting at a particle radius (R). This is not insignificant. More generally a simple scaling of the Coulomb force (F_c) to weight (mg) predicts this ratio scales as $\sim 1/gR$. Similarly to other electrostatic phenomena, the torques generated by inhomogeneous charge will increase as one considers smaller particles or reduced gravity. Our results illustrate that the magnitude of the torque is such that isolated particles may respond to one another, undergoing large rotations. Similarly, particles in a cluster would exert torques upon one another, rotating when subjected to agitation. Since this torque brings oppositely charged regions closer together, the electrostatic forces are strongly amplified increasing the attraction between particles.

Author Contributions

M.R.S and M.I.S both designed and conducted the experiments, built the model, performed the analysis and wrote the paper.

Conflicts of interest

There are no conflicts to declare.

Data Availability

The data analysis scripts of this article are available at https://github.com/mikesmithlab/Charge_Statics_charging_paper

Acknowledgements

We thank D. Laird for technical support in building the apparatus and P.J. Moriarty for useful discussions.

Notes and references

- 1 J. Baptiste, C. Williamson, J. Fox, A.J. Stace, M. Hussan, S. Braun, B. Stamm, I. Mann, E. Besley, *Atmos. Chem. Phys.*, 2021, **21**, 8735–8745.
- 2 S. Pollastri, E. Rossi, C. Bonadonna, *Sci. Adv.*, 2022, **8**, 1–9.
- 3 L. Xie, J. Li, Y. Liu, *Theor. Appl. Mech. Lett.*, 2020, **10**, 276–285.
- 4 A. Mehrotra, F.J. Muzzo, T. Shinbrot, *Phys. Rev. Letts*, 2007, **99**,.
- 5 M. Maamar, T. Zeghoul, W. Aksa, S. Touhami, I. Achouri, L. Dascalescu, *J. Electrostat.*, 2022, **115**,.
- 6 M. Mirkowska, M. Kratzer, C. Teichert, H. Flachberger, *BHM*, 2016, **161**, 359–382.
- 7 G. Hendrickson, *Chem. Eng. Sci.*, 2006, **61**, 1041–1064.
- 8 Y. Pu, M. Mazumder, C. Cooney, *J. Pharm. Sci.*, 2009, **98**, 2412–21.
- 9 H. Kawamoto, A. Shigeta, M. Adachi, *J. Pharm. Sci.*, 2009, **29**, 04015031.
- 10 J.S.M. Harper, G.D. McDonald, J. Dufek, M.J. Malaska, D.M. Burr, A.G. Hayes, J. McAdams, J.J. Wray, *Nat. Geosci.*, 2017, **10**, 260–265.
- 11 D.J. Scheeres, C.M. Hartzell, P. Sánchez, M. Swift, *Icarus*, 2010, **210**, 968–984.
- 12 Y. Sun, Q. Yuan, J. Xiong, *J. Phys.: Conf. Ser.*, 2013, **418**,
- 13 X. Wang, J. Schwan, H.W. Hsu, E. Grün, M. Horányi, *Geophys. Res. Letts.*, 2016, **43**, 6103–6110.
- 14 Wagner, S.A., *The apollo experience: lessons learnt for constellation lunar dust management*, NASA Technical Report NASA/TP-213726, 2006.
- 15 Calle, C.J. and Mackey, P.J. and Hogue, M.D. and Johansen, M.R. and Yim, H. and Delaune, P.B. and Clements, J.S., *J. Electrostat.*, 2013, **71**, 257–259.
- 16 Ball, P., *Nat. News*, 2007.
- 17 V. Lee, S. Waitukaitis, M.Z. Miskin, H.M. Jaeger, *Nat. Phys.*, 2015, **11**, 733–738.
- 18 E.B. Lindgren, B. Stamm, Y. Maday, E. Besley, A.J. Stace, *Phil. Trans. R. Soc. A*, 2018, **376**, 1–20.
- 19 D.J. Lacks, T. Shinbrot, *Nat. Rev. Chem.*, 2019, **3**, 465–477.
- 20 M. Sow, R. Widenor, A. Kumar, S.W. Lee, D.J. Lacks, R.M. Sankaran, *Angew. Chem. Int. Ed.*, 2012, **124**, 2749–2751.
- 21 O. Tilmantine, T. Zeghloul, K. Medles, L. Dascalescu, A. Fatu, *J. Electrostat.*, 2022, **115**, 103651.
- 22 H.T. Baytekin and B. Baytekin and J.T. Incorvati and B.A. Gryzbowski, *Angew. Chem. Int. Ed.*, 2013, **51**, 4843–4847.
- 23 Y. Fang and L. Chen and Y. Sun and W. P. Yong and S. Soh, *J. Phys. Chem.*, 2018, **122**, 11414–11421.
- 24 G. Grosjean and S. Waitukaitis, *Phys. Rev. Letts*, 2023, **130**, 098202.
- 25 H. Grosshans and M.V. Papalexandris, *Powder Technol.*, 2017, **305**, 518–527.
- 26 F. Chowdury and M. Ray and A. Sowinski and P. Mehrani and A. Passalacqua, *Powder Technol.*, 2021, **389**, 104–118.
- 27 T. Steinpilz and K. Joeris and F. Jungmann and D. Wolf and L. Brendel and J. Teiser and T. Shinbrot and G. Wurm, *Nat. Phys.*, 2020, **16**, 225–229.
- 28 B. Andreotti and Y. Forterre and O. Pouliquen, *Granular Media*, Cambridge University Press, 2013, pp. 24–25.

- 29 Y. Zhang and T. Pähntz and Y. Liu and X. Wang and R. Zhang and Y. Shen and R. Ji and B. Cai, *Phys. Rev. X*, 2015, **5**, 011002.
- 30 K.S. Moreira and D. Lermen and Y.A. Santos da Campo and L.O. Ferreira and T.A.L. Burgo, *Adv. Mater. Int.*, 2020, **7**, 2000884.
- 31 C. Heinert and R.M. Sankaran and D.J. Lacks, *J. Electrostat.*, 2020, **105**, 103450.
- 32 J.M. Harper and C.S. McDonald and E.J. Rheingold and L.C. Wehn and R.E. Bumbaugh and E.J. Cope and L.E. Lindberg and J. Pham and Y. Kim and J. Dufek and C.H. Hendon, *Matter*, 2024, **7**, 266–283.
- 33 T. Shinbrot and T.S. Komatsu and Q. Zhao, *EPL*, 2008, **83**, 24004.
- 34 T. Pähntz and H.J. Hermann and T. Shinbrot, *Nat. Phys.*, 2010, **6**, 364–368.
- 35 R. Yoshimatsu and N.A.M Araújo and G. Wurm and H.J. Hermann and T. Shinbrot, *Sci. Rep.*, 2017, **7**, 39996.
- 36 F. Jungmann and T. Steinpilz and J. Teiser and G. Wurm, *J. Phys. Commun.*, 2018, **2**, 095009.
- 37 T. Noguchi and others, *Science*, 2011, **333**, 1121–1125.
- 38 J.Q. Feng, *Phys. Rev. E*, 2000, **62**, 2891–2897.